RESEARCH PAPER

Investigating nanoformulations for the oral delivery of resveratrol to inhibit first-pass metabolism and enhance drug bioavailability

Akram Hassanpour[1], Omid Sabzevari[2], Banafsheh Kiani-Dehkordi[3], Amir Amani[4], Fariba Esmaeili[1], Sharmin Kharrazi[*1]

[1] *Department of Medical Nanotechnology, School of Advanced Technologies in Medicine, Tehran University of Medical Sciences, Tehran, Iran*
[2] *Department of Toxicology and Pharmacology, Faculty of Pharmacy, and Toxicology & Poisoning Research Center, Tehran University of Medical Sciences, Tehran, Iran*
[3] *Department of Pharmaceutics, School of Pharmacy, Tehran University of Medical Sciences, Tehran, Iran*
[4] *Natural Products and Medicinal Plants Research Center, North Khorasan University of Medical Sciences, Bojnurd, Iran*

ABSTRACT

Objective(s): Poor oral bioavailability remains a major barrier for the development of many therapeutic agents, underscoring the need for advanced delivery systems. This study aimed to design and evaluate novel nanoformulations of resveratrol (RSV) to improve its absorption and investigate their effects on CYP3A4 inhibition in rats and enhancing simvastatin bioavailability**.**

Materials and Methods: An oil-in-water nanoemulsion incorporating RSV were synthesized in the oil phase (NE-RSV) and resveratrol-coated gold nanoparticles as a water-soluble form (GNP-RSV). Accordingly, a combined formulation (NE-RSV + GNP-RSV) with maximum RSV loading was prepared and physicochemically characterized. Particle size was measured using Dynamic Light Scattering, and cytotoxicity was assessed on Caco-2 cells via MTT assay. Transport studies across Caco-2 monolayers were performed to examine P-glycoprotein (P-gp) inhibition. Protein expression of CYP3A was assessed through Western blot analysis within liver microsomal preparations. Simvastatin bioavailability in rats was quantified using HPLC following 7-day oral administration. Hematological and biochemical safety markers were also analyzed.

***Results*:** Mean particle sizes were 11.3 ± 6.8 nm for NE-RSV, 22.7 ± 14.3 nm for GNP-RSV, and 36.4 ± 23.0 nm for the combined system. Cytotoxicity results showed no significant reduction in cell viability. Permeability assays confirmed P-gp inhibition. The combined formulation increased simvastatin AUC_{0-24} by 2.7-fold and Cmax by 3.05-fold versus controls, with no adverse changes in blood parameters or liver enzymes at 300 mg/kg.

***Conclusion*:** Nanoformulation of resveratrol led to a measurable increase in oral exposure, supporting its applicability for improving absorption of compounds with solubility-limited bioavailability.

Keywords: *CYP3A; Resveratrol; Nanoemulsion; Pharmacokinetic; Oral delivery*

How to cite this article

Hassanpour A, Sabzevari O, Kiani-Dehkordi B, Amani A, Esmaeili F, Kharrazi Sh. Investigating nanoformulations for the oral delivery of resveratrol to inhibit first-pass metabolism and enhance drug bioavailability. Nanomed J. 2026; 13(3): 469-485. DOI: 10.22038/nmj.2026.92596.2345

INTRODUCTION

Oral delivery is widely utilized in pharmaceutical research due to its high patient compliance, ease of formulation implementation, and effective therapeutic outcomes among the different administration routes (1). Despite significant advances in drug discovery, only 10–20% of lead candidates effectively reach the market (2). Inadequate oral bioavailability and suboptimal pharmacokinetic (PK) performance account for nearly half of clinical development failures among the major causes of attrition (3). Oral drug delivery is frequently limited by pre-systemic metabolism in the intestinal epithelium and liver, which can substantially diminish systemic drug concentrations and generate notable variability in pharmacological response in patients. Among the key molecular determinants, cytochrome P450 enzymes (CYPs) and P-glycoprotein (P-gp) act synergistically to modulate drug metabolism and efflux, further influencing oral bioavailability and interpatient variability (Fig. S1).

Resveratrol has been shown to inhibit both CYP3A4 and P-gp as a naturally occurring

* *Corresponding author:* Sharmin Kharrazi, Associate Professor, Department of Medical Nanotechnology, School of Advanced Technologies in Medicine (SATiM), Tehran University of Medical Sciences (TUMS), Tehran 1417755469, Iran. Phone: +98 2143052135, Fax: +98 21 88991117, Email: sh-kharrazi@tums.ac.ir.

Note. This manuscript was submitted on November 08, 2025; approved on December 29, 2025.

polyphenol, offering a dual mechanism to enhance drug absorption (4,5,6,14).

Resveratrol has been shown to modulate multiple biological pathways, exerting effects that span inflammation control, tumor suppression, neuroprotection, cardiovascular support, glucose regulation, aging modulation, and rheumatologic benefit (5,6). However, the clinical utility of resveratrol is severely restricted due to extremely low oral bioavailability (<1%), rapid metabolism, photosensitivity, low aqueous solubility (0.03 g/L), and a short plasma half-life despite these promising characteristics (7). These limitations have motivated the adoption of nanoscale-based delivery platforms to improve oral exposure and reduce first-pass metabolic effects. Nanoemulsions can improve the water solubility, stability, and bioaccessibility of hydrophobic compounds while protecting them from harsh gastrointestinal conditions. Enhanced lipid digestion kinetics combined with suppression of ATP-linked efflux processes contribute to greater intestinal uptake of poorly soluble molecules, with paclitaxel serving as a representative example (8). Oil-in-water (O/W) nanoemulsions represent a highly favorable platform for resveratrol administration, owing to their straightforward formulation process but they allow drug loading only in the oil phase, limiting the total achievable loading capacity (9,10).

peptides, proteins, and natural compounds GNPs have emerged as versatile drug-delivery platforms owing to their excellent biostability and ability to transport diverse therapeutic agents including nucleic acids (21, 22).

Functionalization and coating of AuNPs strongly influence biodistribution, cellular uptake, and cytotoxicity (10, 13, 14, 15).

Resveratrol-coated AuNPs, offer potential advantages including improved stability, reduced cellular interactions, and enhanced clearance with their polyphenolic shell, making them promising carriers for oral delivery (14,15).

Significant efforts have been directed toward improving the delivery performance of resveratrol through nanoscale formulation strategies (16–19). Despite these advancements, most previous studies have remained confined to single-system designs, leaving more integrated delivery concepts largely unexplored. In contrast, the present study introduces a dual nanoformulation that integrates an oil-in-water nanoemulsion with resveratrol loaded in the oil phase and resveratrol-coated gold nanoparticles dispersed in the aqueous phase. This combined system improves overall loading, phase stability, and the simultaneous contribution of two complementary mechanisms of CYP3A4 and P-gp inhibition. No prior reports have evaluated such a dual-carrier strategy for oral delivery of resveratrol, representing a clear innovation relative to previously published formulations. Simvastatin (SV) a CYP3A4 substrate with poor aqueous solubility and low oral bioavailability was selected as a model drug to assess the pharmacokinetic effects of these nanoformulations (20). Importantly, no in vivo pharmacokinetic studies have previously examined simvastatin using this dual nanoformulation approach. Advanced dispersion-based formulations have been reported to improve the intestinal uptake of lipophilic statins, including atorvastatin (32). This study aimed to create a more efficient oral delivery system by incorporating resveratrol into both nanoemulsions and GNPs, which improves resveratrol stability, facilitates CYP3A4 inhibition, and enhances the bioavailability and therapeutic efficacy of simvastatin (Fig.1).

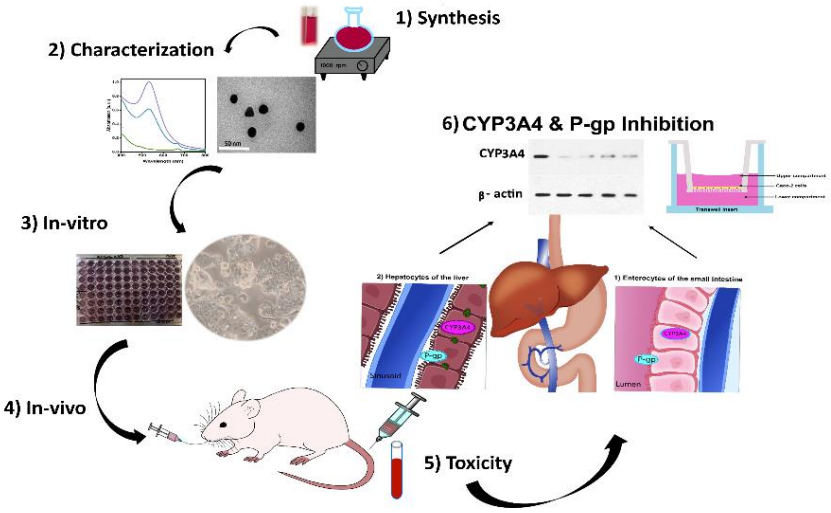

Fig. 1. Graphical abstract summarizing the study features.

MATERIALS AND METHODS

All the applied methods, techniques and materials are explained here.

Green approach for producing resveratrol-stabilized gold nanoparticles: synthesis and physicochemical evaluation

Resveratrol-coated gold nanoparticles (GNP-RSV) were prepared using an environmentally benign synthetic approach (2). Briefly, trans-resveratrol (2 mg; 98% purity; Ly-Health Corporation, China) was freshly dissolved in an aqueous sodium hydroxide solution (0.2 mM; Merck, Germany), which was then promptly introduced into 10 mL of an aqueous chloroauric acid solution (0.1 M $HAuCl_4 \cdot 3H_2O$; Sigma, Germany) under continuous stirring. Reaction conditions were controlled at room temperature (≈25 °C), during which sustained agitation was applied for 120 minutes. Formation of GNP-RSV was confirmed by appearance of characteristic red-wine color. Nanoparticle identity was further validated using UV–visible spectroscopy (Cecil BioAquarius CE 7250, UK), and TEM imaging was used at 100 kV to characterize nanoparticle size and structure.

Preparation and characterization of Nanoemulsion containing Resveratrol (NE-RSV)

Low energy emulsification techniques were used to produce thermodynamically stable nanoemulsions (1). Resveratrol (20 mg) was dispersed in grape seed oil (2.5% w/w; Decamond Chemistry, Esfahan, Iran), after which polysorbate 80 (Tween 80, 17% w/w; Merck, Germany) and water (~80% w/w) were sequentially incorporated. The formulation underwent continuous agitation for one hourunder controlled heating at 60 °C, leading to the generation of a clear and homogeneous system consistent with nanoemulsion development. Particle size characteristics were derived from scattering-based measurements on a Scatter Scope instrument (K-One, South Korea). Surface charge was evaluated independently through electrophoretic mobility analysis using a Horiba SZ-100 system (Horiba Ltd., Japan).

Preparation and characterization of Resveratrol nanoformulation (NE-RSV + GNP-RSV)

A new resveratrol nanoformulation was made by mixing NE-RSV and synthesizing GNP-RSV in a 1:1 (w/w) ratio to load GNP-RSV into the water phase of NE-RSV and hence load RSV into both the water phase and oil phase of the nanoemulsion. NE-RSV+GNP-RSV was characterized by UV-Vis absorption spectroscopy, DLS, zeta potential and TEM.

Stability of Resveratrol nanoformulations

Formulations were monitored for stability over a 30-day period at 4, 25, and 45 °C. NE-RSV and NE-RSV+GNP-RSV samples were prepared by dilution with deionized water to assess their average droplet size prior to DLS measurement. PDI values of droplet size variability, ranged from 0.05 to 0.7 (21), indicating a fairly uniform distribution. Changes in average particle size and stability were tracked for GNP-RSV using UV–Vis spectroscopy.

Cell culture and cytotoxicity assessment

Caco-2 human colonic adenocarcinoma cells (Iranian Biological Resource Center, Tehran, Iran) were propagated in high-glucose Dulbecco's Modified Eagle Medium (DMEM/F-12; GIBCO/BRL Invitrogen, Carlsbad, California), enriched with 10% fetal bovine serum (FBS; GIBCO/BRL Invitrogen, Carlsbad, California) and supplemented with penicillin (100 units/mL) and streptomycin (100 mg/mL; Biosera, England). The cultures were maintained at 37 °C in a humidified incubator with 5% CO_2, ensuring optimal growth conditions. The Caco-2 cells were detached enzymatically using trypsin (Biosera, England) and distributed into 96-well plates to reach a final seeding of 5×10^4 cells per well once reaching confluence. The culture medium was replaced with fresh medium containing resveratrol in its various formulations at concentrations ranging from 1 to 2 mM after allowing the cells to adhere, ensuring uniform exposure across all wells. The removal of the culture medium was performed carefullyfollowing a four-hour exposure, and residual compounds were eliminated by rinsing the cells with PBS (Sigma-Aldrich, USA). The assay proceeded by introducing 10 µL of MTT reagent (5 mg/mL; 98%, Sigma-Aldrich, USA) to each well, allowing for three hours of formazan crystal development under standard laboratory conditions. The medium was discarded after incubation, and 100 µL of DMSO (C_2H_6OS, 99.5%, Sigma-Aldrich, USA) was added to solubilize the crystals. Cellular viability was assessed by recording absorbance at 570 nm (22).

Transwell permeability assay

Caco-2 cells (passage 50 ± 8) were maintained in DMEM/F-12 medium, enriching with 10% FBS and 1% penicillin-streptomycin under a humidified atmosphere containing 5% CO_2 at 37 °C and preparing them for subsequent permeability experiments. Cells were plated onto Transwell

polycarbonate inserts (0.4 µm pore size) for the assays, at a seeding density of 1×10^5 cells per insert and cultured for approximately 25 days to allow the formation of a confluent monolayer. Treatment was initiated when the monolayers demonstrated adequate integrity, as evidenced by transepithelial electrical resistance (TEER) values above 300 Ω/cm². Incubations were performed in Hanks' buffer (Merck, Germany) with 25 mM HEPES (Merck, Germany) at 37 ºC. Treatment groups, comprising NE-RSV+GNP-RSV, NE-RSV, RSV (0.5 mM), and GNP-RSV (matched to the volume present in NE-RSV+GNP-RSV), were introduced into the upper chamber and incubated with the cells for 30 minutes. Simvastatin (Granules India Limited, India) was administered at 40 µM after washing the monolayers with buffer. The sample was withdrawn at times 0.5, 1 and 2 h from the lower compartment for analysis by UV-visible detection. The apparent permeability coefficient (Papp) was determined using equation 1, and a P_{app} value of 0.5*10-6 cms^{-1} was considered acceptable (23).

$$\mathbf{P_{app}} = \frac{\mathbf{dQ}}{\mathbf{dt}} \times \frac{\mathbf{1}}{\mathbf{A\,C_0}} \qquad \text{Eq. 1}$$

Where dQ/dt represents the rate at which the product appears in the basal (A–B) compartment over time, expressed in nmol/s.

A denotes the surface area of the Transwell insert, which is measured in cm².

C_o corresponds to the initial concentration of the product applied to the apical (A–B) compartment, in nmol/mL.

Animal study

Male and female Wistar albino rats, aged 6 weeks and weighing 200 ± 40 g, were sourced from Tehran University of Medical Sciences. The animals were maintained under controlled laboratory conditions, including a temperature of 23 °C, 55% relative humidity, and a 12-hour light/dark cycle, with unrestricted access to food and water. All experimental protocols received approval from the Ethics Committee of Tehran University of Medical Sciences (IR.TUMS.MEDICINE.REC.1400.990). All experimental procedures complied with the applicable institutional guidelines and regulations. The rats underwent random assignment into five groups, including NE-RSV+GNP-RSV, NE-RSV, GNP-RSV, RSV, and control following an acclimation period.

Toxicity (in vivo)

Acute toxicity in the animals was evaluated via oral delivery, employing a stainless-steel feeding needle, with a single 300 mg/kg dose of RSV administered in various formulations: nanoemulsion containing RSV (NE-RSV), nanoemulsion (NE), and nanoemulsion containing resveratrol and RSV coated gold nanoparticle (NE-RSV+GNP-RSV). A 12-hour fasting regimen was implemented for all animals prior to the single-dose administration. Then, they were allowed refeeding with two hours. Baseline body weights were documented for each rat, followed by subsequent recordings on days 7 and 14 using an electronic balance (Fig. 2), thereby enabling a continuous evaluation of weight variations throughout the experimental period. Anesthesia was achieved in the rats through intraperitoneal administration of ketamine (100 mg/kg) combined with xylazine (10 mg/kg). Blood was obtained via cardiac puncturefollowing anesthesia, and the collected samples were analyzed with a KX-21 hematology analyzer (Kobe, Japan) to determine hematological parameters. Blood analysis encompassed multiple hematological parameters. Red blood cell indices, including RBC count, hemoglobin content (HGB), hematocrit (HCT), mean corpuscular volume (MCV), mean corpuscular hemoglobin (MCH), and mean corpuscular hemoglobin concentration (MCHC), were evaluated, alongside white blood cell counts (WBC) with differential assessment of neutrophils (NEUT) and lymphocytes (LYM), as well as platelet (PLT) levels.

Liver and kidney functions were determined from serum samples by measuring aspartate aminotransferase (AST), alanine transaminase (ALT), and alkaline phosphatase (ALP) using commercial enzymatic colorimetric kits (Randox Analytical, UK).

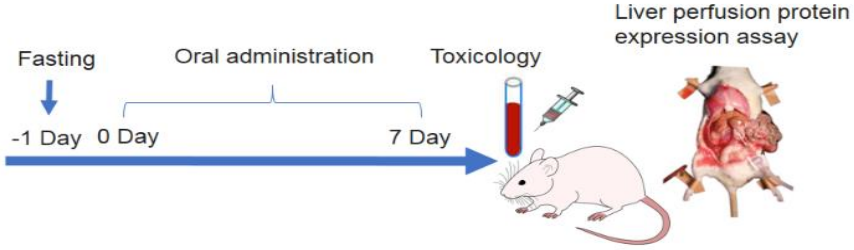

Fig. 2. Timeline of the animal studies.

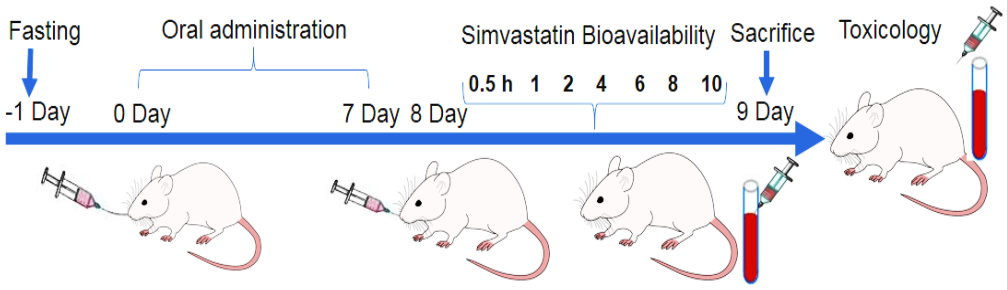

Fig. 3. In vivo assessment timeline of Simvastatin bioavailability.

Western blotting

The western blotting technique was appliedto assess the protein expression assay in microsomes. The animals were starved the night before the treatment. Animals received various nanoformulations by gavage, each providing an RSV-equivalent dose of 80 mg/kg for seven consecutive days. On day eight, rats were anesthetized via intraperitoneal injection of ketamine hydrochloride (100 mg/kg) combined with xylazine hydrochloride (10 mg/kg). Once anesthesia was established, circulating blood was withdrawn for analysis, and the livers were perfused and immediately frozen at −80 °C for subsequent microsome preparation (Fig. 3).

Liver microsomal proteins from individual rats were prepared by mixing with a loading buffer containing 0.125 M Tris (pH 6.8), 20% glycerol, 10% β-mercaptoethanol, 4% SDS, and 0.004% bromphenol blue. A total of 10 µg of protein per lane underwent denaturation by heating at 95 °C for 5 minutes, followed by separation on 12% SDS–PAGE gels and subsequent transfer onto polyvinylidene fluoride (PVDF) membranes (Merck Millipore, Darmstadt, Germany). Membranes were subsequently blocked with 5% non-fat milk in Tris-buffered saline containing 0.08% Tween 20 for 1 h at room temperature, and incubated overnight at 4 °C with primary antibodies (Santa Cruz Biotechnology, USA). Following the washing step, membranes underwent incubation with the respective secondary antibodies for one hour at room temperature. β-Actin (Santa Cruz Biotechnology, USA) was utilized as the loading control. Chemiluminescent was detected using Immobilon Western HRP Substrate (Millipore, Watford, GBR), and signal acquisition was carried out on a Fusion SL imaging system (Vilber Lourmat, Germany). Quantification of band intensities was achieved using ImageJ software (version 1.48, NIH, Bethesda, USA).

Pharmacokinetic study

Pharmacokinetic of simvastatin was assessed in blood plasma in five study groups NE-RSV+GNP-RSV, NE-RSV, GNP-RSV, RSV, and Control (water). Prior to dosing, the rats underwent a 12-hour fasting period, followed by daily oral administration of nanoformulations equivalent to 80 mg/kg RSV for seven days. On the eighth day, all animals received a single oral dose of simvastatin (20 mg/kg body weight). Anesthesia was achieved through intraperitoneal injection of ketamine (100 mg/kg) together with xylazine (10 mg/kg), and a minor longitudinal incision was performed above the right jugular vein to facilitate vascular access. The vein was carefully isolated by blunt dissection and catheterized using laboratory-grade tubing. The cannula permitted repeated blood collection while minimizing stress and damage to surrounding cellular structures. At the specified time intervals (0, 1, 2, 4, 6, 8, 10, and 24 h), approximately 0.5 mL of blood was obtained from each rat and immediately aliquoted into heparin-coated 1.5 mL microcentrifuge tubes (Fig. 3). Samples were centrifuged at 5000 rpm for 20 minutes, and simvastatin levels in the plasma were quantified using HPLC-UV (Knaver Smartline Pump 1000 with UV detector 2600, Germany). In brief, 50 µl of simvastatin solution as internal standard and 100 µl of acetonitrile were added to precipitate the proteins to 100 µl of plasma sample. The mixture was vortex mixed for 10 min and then centrifuged at 12,000 rpm for 10 min. A 250 µL aliquot of the supernatant was transferred to a fresh microtube and centrifuged at 12,000 rpm for 10 min. Subsequently, 100 µL of the resulting supernatant was introduced into the HPLC system for analysis. The UV detector was operated at 239 nm, and the column (Tracer Excel 120 ODSA, 5 µm, 15 × 0.46 cm; Teknokroma) was maintained at 25 °C throughout the run. The flow rate was 1.4

ml/min, and the mobile phase consisted of acetonitrile, H2O (pH: 4), in a ratio of 1:2, 75:25 (v/v/v).

The HPLC run lasted 7 minutes, with simvastatin eluting at 5 minutes. Quantification relied on a calibration curve generated from plasma standards (10–1000 ng/mL), and the method was validated for linearity, accuracy (> 95%), and precision, with intra- and inter-day RSD values below 5%.

Statistical Evaluation

Experiments were conducted in triplicate, and data are expressed as mean ± standard deviation. Statistical analyses were performed using one-way ANOVA with LSD post hoc comparisons, and differences were considered significant. Graphs were generated using Origin 2019.

Ethics Approval and Animal Experimentation Consent

The use of animals in all experiments was conducted following national and institutional guidelines for laboratory animal care. Study protocols received approval from the Animal Ethics Committee of Tehran University of Medical Sciences (Approval No. IR.TUMS.MEDICINE.REC.1400.990).

RESULTS

Preparation and characterization of resveratrol nanoformulations

Resveratrol-coated gold nanoparticles (GNP-RSV) were prepared using a green synthesis approach (Fig. 4A, B, and E) and exhibited a characteristic SPR band at 532 nm. Post-synthesis nanoparticles were subjected to repeated washing using Amicon® ultrafiltration tubes, and the filtrate was subsequently assessed by UV–Vis spectrophotometry. The presence of a strong absorption peak attributed to RSV in the spectrum confirmed the formation of GNP-RSV (Fig. S4). No resveratrol signal was observed in the filtrate, suggesting that the concentration of unbound resveratrol fell below the instrument's detection threshold. These results indicated that nearly the entire amount of resveratrol was effectively conjugated to the gold nanoparticles. A low-

Energy method was employed to prepare a stable nanoemulsion. Briefly, resveratrol was dissolved in oil and surfactant (Tween 80). Water was gradually introduced in a dropwise manner once the solution achieved clarity. The formation of a transparent solution effectively prepared the nanoemulsion (Fig. 4C, D). Such optical clarity and absence of precipitation are widely accepted as reliable indirect indicators of complete drug loading, especially for lipophilic compounds like resveratrol in oil- in- water nanoemulsion systems.

Equal volumes of the nanoemulsion containing resveratrol (NE-RSV) and resveratrol-coated gold nanoparticles (GNP-RSV) were mixed for the final formulation, and the resulting formulation was named NE-RSV+GNP-RSV. This volume ratio resulted from various optimization experiments. The UV-Vis absorption spectra of all RSV-containing formulations are depicted in Fig. 4E.

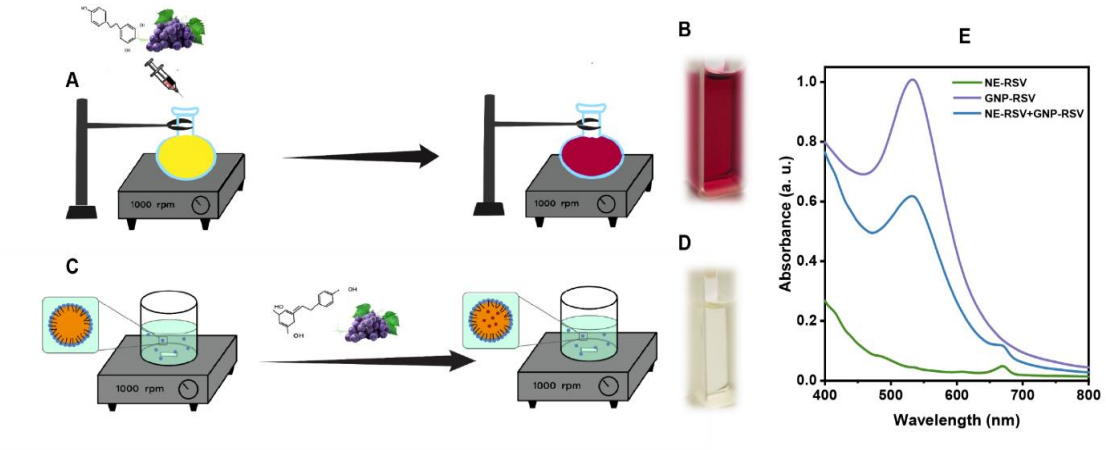

Fig. 4. Schematic diagram of synthesis of resveratrol-coated gold nanoparticles (GNP-RSV) (A) and its wine-red color colloidal solution (B), Schematic diagram of prepring nanoemulsion containing resveratrol (NE-RSV) (C) and its clear appearance (D) and UV-visible absorption spectra of nanoemulsion containing resveratrol + resveratrol-coated gold nanoparticles (GNP-RSV+NE-RSV) (E).

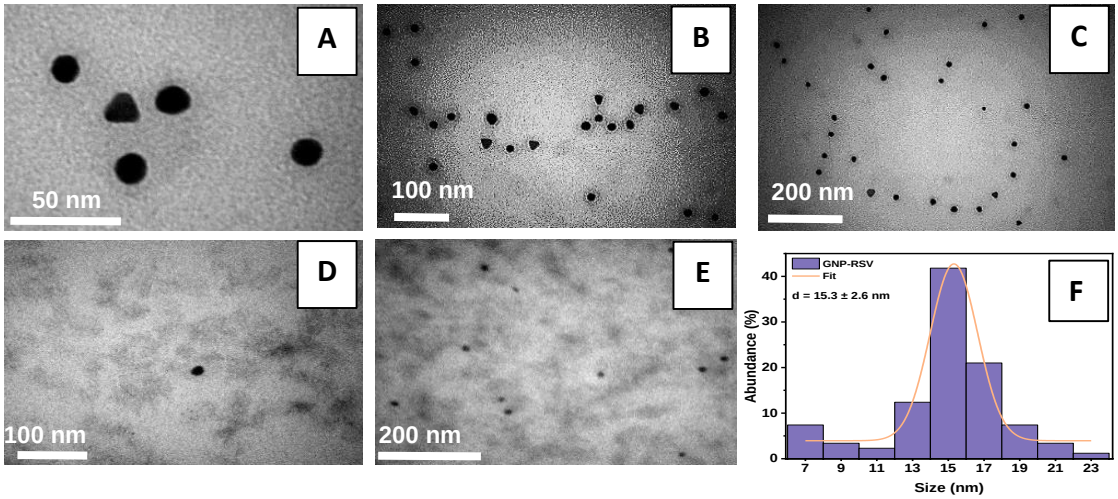

Fig. 5. TEM Micrographs of resveratrol coated gold nanoparticles (GNP-RSV) (A, B, C) nanoemulsion containing resveratrol + resveratrol coated gold nanoparticles (NE-RSV+GNP-RSV) (D, E) and the size distribution histogram of GNP-RSV (F).

Dynamic light scattering (DLS) was employed to characterize the particle size and size distribution of the nanoformulations (Fig. S3). According to DLS and zeta potential results, the size distribution and zeta potential of the formulations was 11.3±6.8 nm (NE-RSV) and -4.9±2.0 mV, 22.7±14.3 nm (GNP-RSV), and 36.4±23.0 nm and 7.2±0.8 mV (NE-RSV+GNP-RSV).

TEM was utilized to study the morphology and the size of GNP-RSV and NE-RSV+GNP-RSV nanoformulations. The TEM micrographs are presented in Fig. 5A-E and the size distribution histogram of GNP-RSV nanoparticles obtained by measuring more than 150 particles was presented in Fig. 5F.

Stability of nanoformulations

Formulations were stored at three different temperatures (4, 25, and 45 °C) for 30 days to evaluate their stability. Prior to measurement, NE-RSV and NE-RSV+GNP-RSV suspensions were prepared by dilution in deionized water. Dynamic light scattering (DLS) was analyzed to determine the sizes of the oil droplets, whereas the polydispersity index (PDI) provided information on the uniformity of particle size distribution. Stability and particle size were additionally examined for GNP-RSV via UV–visible spectroscopy (Tables S1 and S2).

Cytotoxicity assay

The effects of RSV-loaded nanoformulations on the metabolic activity of Caco-2 cells were assessed using the MTT assay. The cytotoxicity of NE-RSV+GNP-RSV, NE-RSV, GNP-RSV, RSV, and NE treatments, was assessed over 4 hours (Fig. 6A), each containing the same concentration of resveratrol and reflecting the short physiological residence time of orally administered formulations in the intestinal tract. Although the results indicated a dose-dependent response in cell viability, no significant toxicity was observed for nanoformulations containing either 1 or 2 mM of RSV. Since 1 mM of RSV showed some level of cytotoxicity and any damage to the cells may alter the permeability test results, the concentration of 0.5 mM resveratrol was chosen for all formulations in the transwell test. Cell viability following simvastatin treatment was assessed (Fig. 6B). Nearly 100% viability was observed at concentrations up to 40 µM.

Effect of pretreatment with resveratrol nanoformulations on transepithelial permeability of simvastatin

Simvastatin movement across the epithelial layer was monitored to determine the effect of pretreatment with RSV nanoformulations on P-glycoprotein function, with the experimental setup shown in Fig. S2. The effects of NE-RSV+GNP-RSV, NE-RSV, GNP-RSV, and free RSV treatments containing 500 µM resveratrol were studied for 30 minutes and compared against a control group with no pretreatment. The resulting values were (6.6±0.1) × 10^{-6}, (8.1±1.0) × 10^{-6}, (3.2±0.3) ×10^{-6}, (6.4±0.5) × 10^{-6}, and (4.6±0.5) × 10^{-6} cm.s^{-1}, respectively (Fig. 7). Apparent permeability coefficient (Papp) values below 1 × 10^{-6} cm.s^{-1} generally reflect low intestinal permeability and, consequently, limited absorption (24). P-gp inhibition was assessed indirectly by measuring the increased apparent permeability (Papp) of simvastatin, a recognized P-gp substrate, traversing

the Caco-2 cell monolayer (25). The rise in Papp values after RSV treatment indicates efflux pump inhibition. The results showed increased permeability with NE-RSV+GNP-RSV and NE-RSV pretreatment compared to the control, suggesting that nanoformulated RSV modulates P-gp (Fig. 7). These findings implied that RSV pretreatment in various nanoformulations may affect simvastatin's permeability and potentially influence its absorption in the intestine (26).

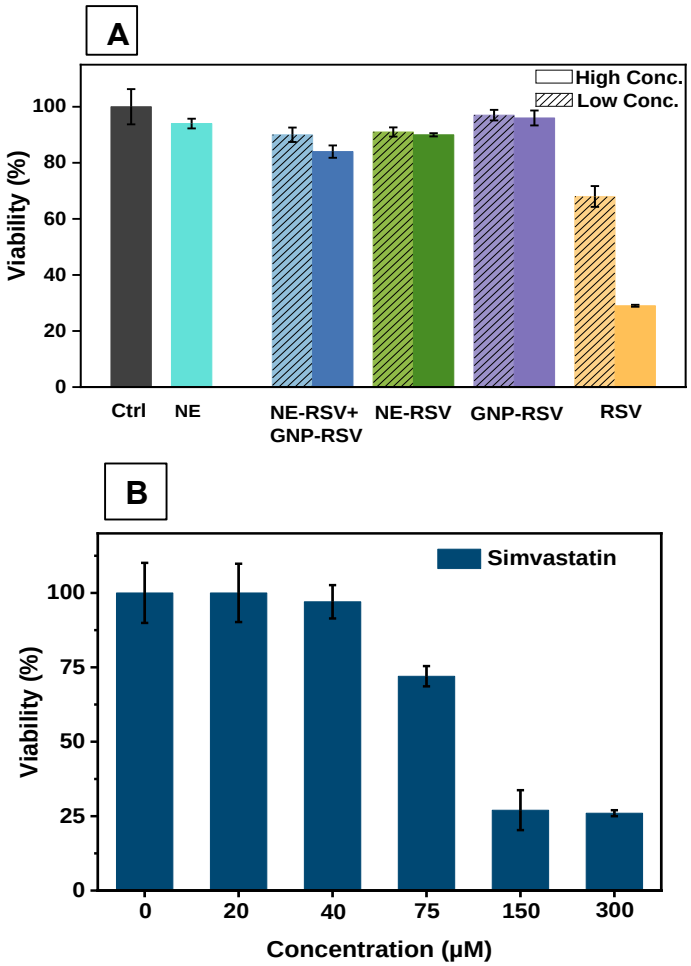

Fig. 6. (A) The percentage of viable Caco-2 cells was determined following a 4-hour exposure to low (1 mM) and high (2 mM) concentrations of resveratrol in the forms of NE-RSV+GNP-RSV, NE-RSV, GNP-RSV, RSV alone, and NE without resveratrol. Similarly, cell viability was assessed after a 4-hour incubation with varying doses of simvastatin. (mean ± standard deviation (n = 5)).

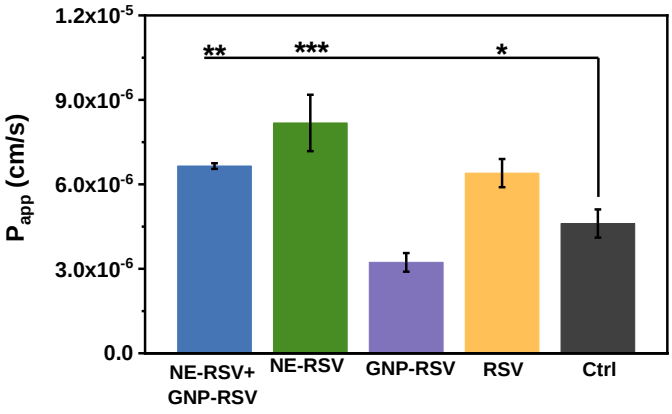

Fig. 7. Apparent permeability of simvastatin determined after NE-RSV+GNP-RSV, NE-RSV, GNP-RSV, RSV, and Ctrl across Caco-2 monolayer (mean ± SD; n=3).

Animal toxicity assessment

The effects of different resveratrol formulations, including NE-RSV+GNP-RSV, NE-RSV, NE, and free RSV in vivo. Animals were monitored closely over a 14-day period for any signs of toxicity or mortality. No adverse events or deaths were observed during the study. Physical observations showed that skin, fur, eyes, and mucous membranes remained normal. Furthermore, no changes in behavior, tremors, excessive salivation, diarrhea, sleep patterns, or signs of coma were noted.

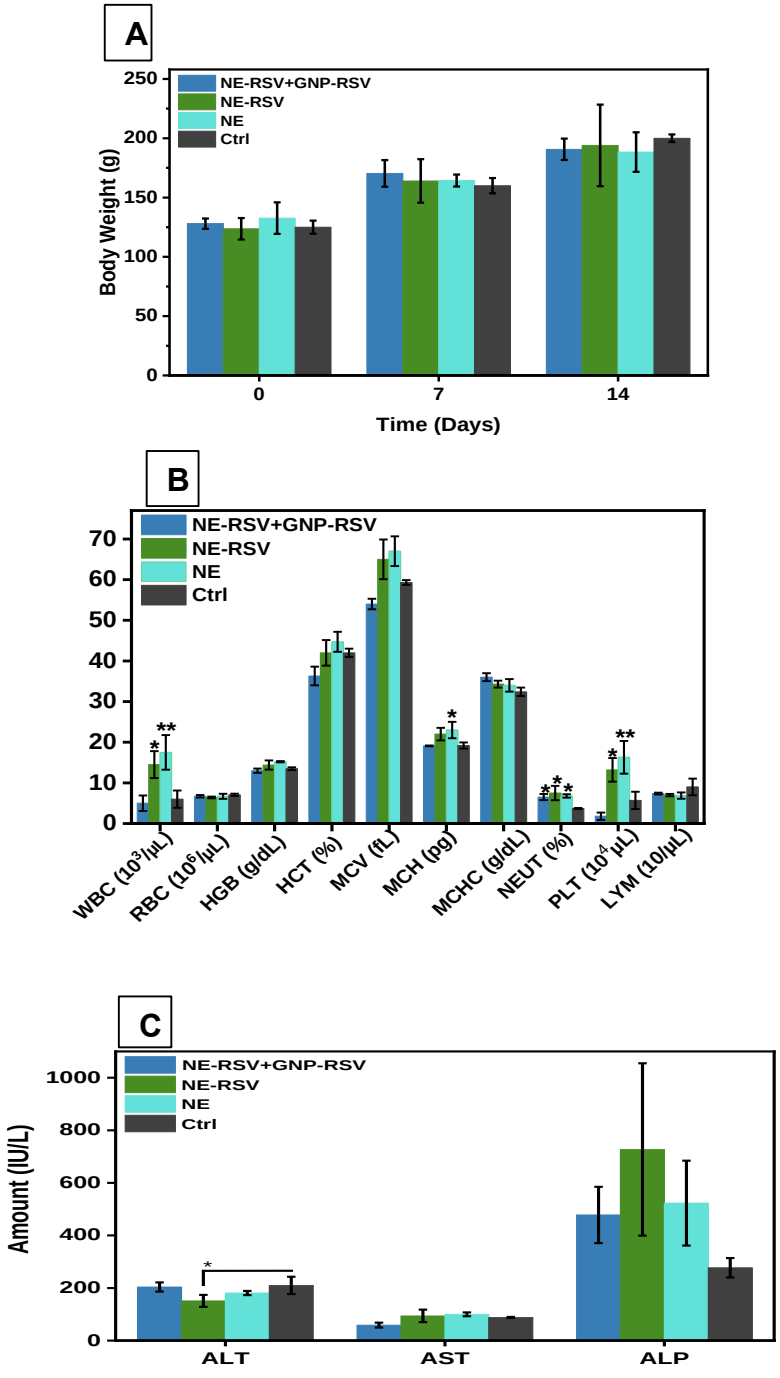

Fig. 8. (A) Body weight was monitored on days 0, 7, and 14, and values were compared with those of the control group (n = 3). (B) Hematological parameters, including WBC, RBC, HGB, HCT, MCV, MCH, MCHC, NEUT, LYM, and PLT, were measured, and results from treated animals were contrasted with controls (n = 3). (C) Serum enzyme activities, namely ALT, AST, and ALP, were determined for all treatment groups and compared to the control animals (n = 3). Data were expressed as mean ± SD, with statistical significance defined as $p < 0.05$ and $p < 0.01$.

As shown in Fig. 8A, body weight increased gradually in all treatment groups, following a pattern similar to that of the control group. After 14 days, hematological analyses were performed to evaluate the impact of resveratrol nanoformulations. Results are summarized in Fig. 8B. Certain parameters showed statistically significant differences compared to controls, including WBC counts in NE-RSV and NE groups, MCH levels in the NE group, neutrophil counts across all treated groups, and platelet numbers in NE and NE-RSV groups. Nevertheless, the majority of hematological parameters stayed within normal limits and exhibited no notable changes relative to controls.

In summary, the data indicated that the tested resveratrol nanoformulations did not induce significant toxicity or mortality in rats, and observed changes in hematological parameters were minimal and unlikely to be biologically relevant.

Liver function tests

Liver function assessments are essential for evaluating the potential toxicity of bioactive compounds or final formulations. As shown in Fig. 8C, none of the treated groups exhibit notable increases in liver function markers. Serum concentrations of key hepatic enzymes were assessed, including ALP (alkaline phosphatase), ALT (alanine aminotransferase), and AST (aspartate aminotransferase). Notably, only the NE-RSV group (resveratrol: 300 mg/kg) exhibited a statistically significant reduction in ALT in comparison with the controls. Nonetheless, this variation is regarded as clinically insignificant, in agreement with previous studies (27,28). Overall, these findings indicated that resveratrol nanoformulations did not induce appreciable liver toxicity, further supporting their safety profile.

CYP3A expression in rat liver

CYP3A expression was evaluated in the livers of rats administered different resveratrol formulations. Mean relative CYP3A expression levels were 0.49, 0.43, and 0.65 in the NE-RSV+GNP-RSV, NE-RSV, and GNP-RSV groups, respectively, relative to controls (Fig. 9A, B). All resveratrol nanoformulations tested induced a significant decrease in CYP3A expression.

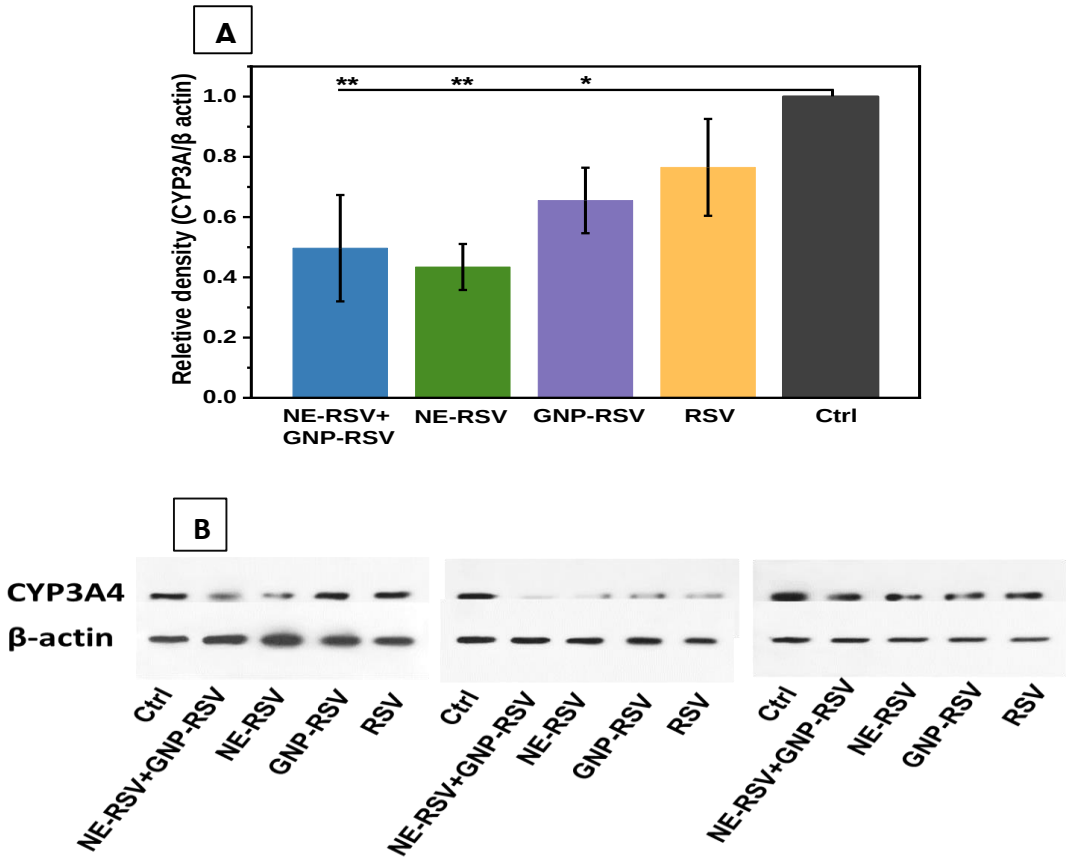

Fig. 9. Western blotting was performed to assess CYP3A levels in liver microsomes of rats treated orally with NE-RSV+GNP-RSV, NE-RSV, GNP-RSV, or RSV. Bar graphs represent the quantified enzyme levels (mean ± SD; n = 3). Representative blot images from each treatment group (NE-RSV+GNP-RSV, NE-RSV, GNP-RSV, RSV, and control) illustrate CYP3A expression, with β-actin used for normalization. Differences compared to the control group were considered significant at $p \leq 0.05$.

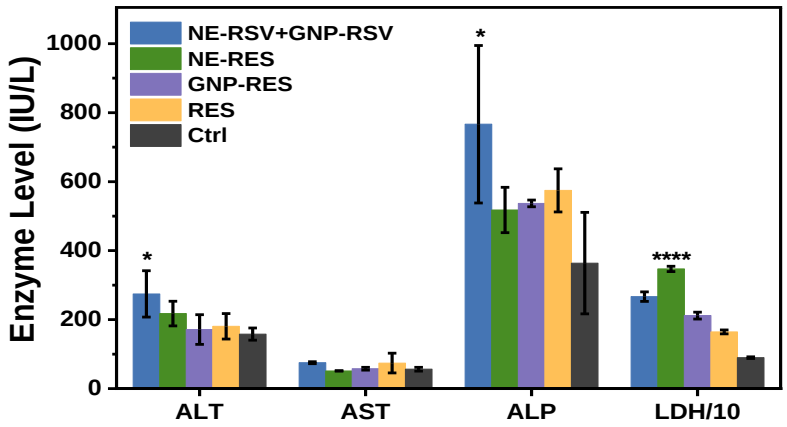

Fig. 10. Effect of daily oral treatments over a period of seven days on serum enzyme activities, including ALT, AST, ALP, and LDH, measured in rats (n = 3). Differences were considered statistically significant at $p < 0.05$

Assessment of liver enzymes

Serum activities of liver enzymes ALT, AST, ALP, and LDH were tracked throughout the study after seven consecutive days of oral resveratrol formulation administration, followed by a single simvastatin dose on day 8 (Fig. 10). LDH activity was significantly increased across all treatment groups, while elevated ALT and ALP levels were specifically observed in rats receiving NE-RSV+GNP-RSV.

Effect of pretreatment with different forms of resveratrol on pharmacokinetics of simvastatin

Figure 11 illustrates the changes of plasma simvastatin concentrations over time following oral administration at 20 mg/kg in rats received 80 mg/kg of different resveratrol formulations prior to dosing. In addition, rats pretreated with the combined nanoformulation (NE-RSV + GNP-RSV) exhibited a significant modification in simvastatin pharmacokinetics ($p \leq 0.05$; Table 1). Pharmacokinetic analysis increased peak plasma concentration (Cmax), the area under the curve until the last measurable point (AUC0–t), and the total extrapolated AUC (AUC0–∞) in animals pre-treated with NE-RSV + GNP-RSV relative to the control group.

Administration of RSV or the combined NE-RSV + GNP-RSV formulation altered the timing of simvastatin's peak plasma levels compared with untreated animals. This observation suggests that the nano-carrier system may enhance the intestinal uptake of simvastatin, potentially leading to improved systemic availability.

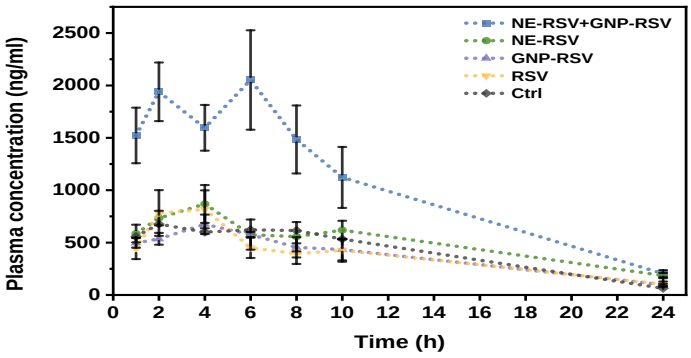

Fig. 11. Rats were administered daily oral doses of NE-RSV + GNP-RSV, NE-RSV, GNP-RSV, or RSV for seven consecutive days, after which plasma concentrations of simvastatin were tracked at designated time points. On day eight, a single simvastatin dose was given. Data were reported as mean ± SD.

Table 1. The effects of daily administration of NE-RSV + GNP-RSV, NE-RSV, GNP-RSV, or free RSV are summarized for one week on simvastatin plasma levels in rats. Results are presented as average values with standard deviation, and * marks indicate statistically significant differences ($p < 0.05$) relative to untreated animals.

Groups	AUC_{0-24} (ng/ml•h)	$T_{½}$ (h)	T_{max} (h)	C_{max} (ng/ml)	AUC_T (ng/ml•h)	AUC_{0-24}/AUC_T (%)
NE-RSV+GNP-RSV	17310.0±3936.1****	6.4±0.65	4.4±1.8	2415.0±963.4***	19043.7±4372.5****	90.9
NE-RSV	7391.6±1467.2	7.5±1.8	4.7±1.1	1085.0±378.41	9463.5±2856.8	78.10
GNP-RSV	6251.6±1906.6	7.1±3.4	4.8±1.1	739.5±272.6	7390.1±1720.5	84.6
RSV	6509.0±2095.6	5.9±0.6	2.5±1	954.2±409.4	7602.2±2654.6	85.6
Ctrl	6389.3±2014.5	6.1±2.6	5.2±2.9	789.3±227.7	6858.4±2842.9	93.2

DISCUSSION

A nanoformulation was designed, synthesized, and characterized containing resveratrol in the form of an oil-in-water nanoemulsion, with resveratrol loaded in the oil phase and resveratrol-coated gold nanoparticles loaded in the water phase (NE-RSV+GNP-RSV). This delivery system and its constituents were applied for the oral administration of RSV, and their effects were studied on inhibiting cytochrome P450 CYP3A and P-gp, as well as the subsequent bioavailability of the model drug in rats. Clinical observations in recent studies have suggested that the pharmacokinetics of drugs co-administered with dietary supplements may be altered by certain flavonoids and plant-derived polyphenols. These herbal compounds exhibit selective interactions with certain CYP450 isoenzymes, thereby influencing the pharmacokinetics and metabolism of drugs processed by these enzymes. Polyphenol-drug interactions may modify drug absorption, distribution, and metabolism, ultimately impacting bioavailability (29,30). The present results suggested that the interplay of natural compounds and conventional medications should be carefully evaluated, as they may alter drug efficacy and increase the risk of adverse reactions. Further studies are needed to clarify the mechanisms behind these observations and develop evidence-based approaches for their clinical application. In the present work, multiple resveratrol-based nanoformulations were prepared, including a resveratrol-loaded nanoemulsion (NE-RSV), gold nanoparticles coated with resveratrol (GNP-RSV), and a hybrid nanodelivery system combining both strategies (NE-RSV+GNP-RSV), which were then compared to free RSV.

The current work evaluated the effect of these nanoformulations on the intestinal uptake of resveratrol. These findings provided strong support that nanoformulations can markedly enhance the oral bioavailability of resveratrol, which may in turn improve its therapeutic potential. The compound's poor solubility in water has been recognized as a primary limitation to its absorption. Nanoemulsion-based delivery systems represent a promising strategy to overcome this barrier, as their submicron droplet architecture markedly increases interfacial surface area, thereby facilitating enhanced gastrointestinal absorption and improving systemic bioavailability (5,31). In this context, the study examined the use of nanoemulsions as an oral delivery system to overcome the limited bioavailability of resveratrol. Exploiting the distinctive physicochemical properties of nanoemulsions can enhance both solubility and intestinal permeability of resveratrol, ultimately supporting improved therapeutic outcomes. The effective formation of the resveratrol nanoemulsion (NE-RSV) was confirmed by the appearance of a clear solution. The physicochemical stability, sustained optical clarity, and absence of precipitation or turbidity observed in NE-RSV strongly indicated that resveratrol was fully solubilized and effectively incorporated into the oil phase of the nanoemulsion. As previously reported, these characteristics serve as reliable indirect indicators of high entrapment efficiency in O/W nanoemulsions, particularly for lipophilic molecules such as resveratrol (32). Additionally, the formation of resveratrol-coated gold nanoparticles was verified by the emergence of a red wine-colored colloidal solution (Fig. 4E). Conjugation efficiency was directly assessed by ultrafiltration using Amicon® filters followed by UV-Vis analysis of the filtrate for the gold nanoparticles (GNP-RSV). No detectable resveratrol was present in the filtrate, confirming that the entire amount of resveratrol had been effectively bound to the gold nanoparticle surface, providing strong evidence of complete drug loading and efficient conjugation in the GNP-RSV system. Measurements by dynamic light scattering and zeta potential analysis indicated that NE-RSV droplets averaged 11.3 ± 6.8 nm with a surface charge of –4.9 ± 2.0 mV, while GNP-RSV particles exhibited a mean size of 22.7 ± 14.3 nm. The combined NE-RSV + GNP-RSV formulation exhibited a larger mean size of 36.4 ± 23.0 nm along with a slightly positive surface charge of +7.2 ± 0.8 mV. These findings indicated that the

nanoformulations were effectively synthesized, and the observed variations in zeta potential and particle size may influence their colloidal stability and biological performance (Fig. S3A–E). TEM imaging showed that the gold nanoparticles predominantly exhibited a spherical shape and uniform size distribution, with a mean diameter of 15 ± 3 nm (Fig. 5A–C, F). The resveratrol coating on the nanoparticle surface was clearly visible in the micrographs. TEM results also verified the uniform dispersion of gold nanoparticles in the water phase of the nanoemulsion (Fig. 5D, E)**.** The use of green synthesis to produce gold nanoparticles (GNPs) with resveratrol resulted in monodispersed and highly stable GNPs. This approach simultaneously enabled resveratrol to be effectively carried by the GNPs, addressing the compound's solubility limitations. By employing this strategy, resveratrol was effectively loaded into the lipid and aqueous fractions of the nanoemulsion, enhancing its overall solubility and potential bioavailability. The sustained optical clarity, absence of precipitation, and stable particle size distribution throughout the storage period provided strong indirect evidence that drug loading and entrapment efficiency remained unchanged over time (33).

Assessing the cytotoxicity of new nanoformulations intended for medical applications is crucial, which helps determine their safety and potential side effects. Caco-2 cells were exposed to each synthesized nanoformulation to assess potential cytotoxic effects (Fig. 6A). Based on the observed cell viability, an appropriate concentration was selected for subsequent permeability studies. Free RSV significantly reduced cell viability when applied at 1 mM. A lower dose of 500 µM RSV was selected for the drug permeability test to preserve epithelial integrity (Fig. 7). This concentration ensures that the cells remain viable and functional while evaluating the effectiveness of the nanoformulations in enhancing drug transport and absorption. The permeability test results demonstrated increased simvastatin permeability in the following treatment groups: NE-RSV+GNP-RSV, NE-RSV, and RSV. As a known substrate of P-gp (34), simvastatin's transport can be influenced by P-gp activity. Research has shown that polysorbate and other surfactants present in nanoemulsions can inhibit P-gp-mediated transport by interacting with the cell membrane, thereby improving oral bioavailability of drugs (31). Some naturally derived compounds, such as resveratrol, have been reported to inhibit P-glycoprotein-mediated efflux (34–39). Consequently, resveratrol nanoformulations may reduce simvastatin efflux by inhibiting P-gp activity. Furthermore, previous studies have indicated that resveratrol enhances simvastatin absorption (40–43). Since simvastatin has a low permeability coefficient (44), pretreatment with resveratrol is expected to enhance its bioavailability. The results indicated that nanoformulations containing resveratrol can markedly improve the oral bioavailability of simvastatin, offering a promising approach to enhance therapeutic efficacy. Additional research is needed to clarify the clinical implications and further optimize the formulation for maximal efficacy.

In this study, a comprehensive animal toxicity of various treatments was assessed (Fig. 8). Most blood parameters did not show significant changes, except for minor alterations in a few parameters, including white blood cells (WBC) in the NE-RSV and NE groups, mean corpuscular hemoglobin (MCH) in the NE group, neutrophils (NEUT) in all three groups, and lymphocytes (LYM) in the NE and NE-RSV groups. As reported in previous studies, these findings do not indicate clinical abnormalities, although some minor changes were observed (28,45).

No mortality or observable clinical signs were noted in any animal group throughout the study, consistent with previous findings that oral resveratrol administration does not induce sub-acute toxicity in rodents (46).

Therefore, the resveratrol nanoformulations developed in this study are well-tolerated and possess a favorable safety profile. Liver enzyme assays conducted after 7 days revealed significant changes in alanine aminotransferase (ALT) and alkaline phosphatase (ALK-P) levels in the NE-RSV+GNP-RSV treated group, as well as lactate dehydrogenase (LDH) levels in all groups, suggesting potential liver-related effects. This study also examined the impact of various resveratrol nanoformulations on cytochrome P450 CYP3A expression in rat liver. In addition, there was a marked downregulation of CYP3A expression following treatment with NE-RSV+GNP-RSV, NE-RSV, and GNP-RSV. Western blot analysis further confirmed that the total P450 protein levels in rat liver microsomes may reflect protein inactivation associated with resveratrol-mediated modulation of gene expression (47).

These results emphasized the possible influence of resveratrol-based nanoformulations on hepatic function and drug metabolism. Simvastatin is commonly used as a model substrate for CYP3A4 in pharmacokinetic studies (48). However, previous research has demonstrated that simvastatin

administration in animals can elevate serum levels of liver enzymes**,** including ALT, AST, ALP**,** and LDH. These elevations are generally associated with drug-induced hepatic structural alterations and the development of necrotic lesions in hepatocytes (49,50). In the present study, increased LDH levels were observed in all RSV-treated rats receiving simvastatin, which is consistent with these prior reports. This finding likely represents an indirect consequence of enhanced simvastatin bioavailability mediated by RSV nanoformulations, rather than direct hepatotoxic effects of the RSV formulations themselves.

Consistently, another study on naringenin found that simvastatin, administered orally once daily at 20 or 40 mg/kg for a continuous period of 30 days, induced elevations in hepatic enzyme levels and caused histopathological changes in the liver of rats (51). Taken together, the minor elevations in LDH observed in this study may increase systemic exposure to simvastatin due to the RSV formulations, rather than inherent toxicity, highlighting the indirect pharmacokinetic interaction rather than a safety concern.

These data support earlier evidence that resveratrol may increase the oral availability of drugs by reducing CYP3A4 and P-glycoprotein activity in both liver and intestinal cells (52–54). The interaction of these enzymes with AuNPs, which can alter their structural conformations, may also contribute to CYP inhibition (55). These results emphasized the significance of assessing interactions between drugs and natural compounds like resveratrol, as well as the impact of nanocarriers such as AuNPs on drug metabolism. Importantly, this study indicated that resveratrol-coated AuNPs exhibit a favorable safety profile: no significant alterations were observed in liver enzyme markers, and permeability assays demonstrated reduced translocation, suggesting minimal tissue accumulation and low acute toxicity. Additional studies are warranted to establish the optimal balance between resveratrol's bioavailability-enhancing effects and the potential hepatotoxic risks when co-administered with simvastatin or other drugs metabolized via similar pathways. Such knowledge develop safer and more effective drug delivery systems, ultimately improving therapeutic outcomes. Previous studies have proposed multiple mechanisms for CYP3A4 inactivation, including the generation of a reactive intermediate by a CYP3A4 substrate within the enzyme's active site, which may impair enzyme activity through modifications of the heme group or the apoprotein structure (6,47). In contrast, the proposed mechanism focuses on altering the enzyme's function rather than its structure (56). Resveratrol can act as a substrate for CYP3A4, potentially leading to enzyme inactivation during the catalytic process. Additional studies on this mechanism offered critical insights into resveratrol–CYP3A4 interactions and optimized drug delivery strategies employing resveratrol nanoformulations. Elucidating how resveratrol suppresses CYP3A4 activity may inform the design of safer and more effective therapies when co-administered with drugs metabolized by this enzyme. The findings indicated that NE-RSV+GNP-RSV can serve as a supplement to inhibit CYP3A4, thereby enhancing drug bioavailability. The results demonstrated a significant improvement in drug bioavailability compared to bulk resveratrol. The observed enhancement likely stems from gold nanoparticles interacting with the enzyme's active site, which reduces its activity. Simultaneously, the nanoemulsion improves intestinal permeability, leading to enhanced drug absorption.

These results underscored the potential of NE-RSV+GNP-RSV as a promising approach to enhance drug bioavailability through CYP3A4 modulation and increased intestinal absorption. Further studies are necessary to refine the formulation, evaluate long-term safety, and investigate its clinical utility for drugs with limited bioavailability. Unlike many nanoformulations relying on high-energy or complex fabrication techniques, such as high-pressure homogenization or ultrasonication, the presented formulation was developed using a low-energy, solvent-free emulsification method, which is simple, reproducible, and highly scalable. The gold nanoparticles were synthesized via a facile aqueous reduction method mediated by resveratrol, without the need for specialized equipment, organic solvents, or inert gas. Therefore, both components of the formulation were prepared using cost-effective and scalable processes, addressing a key limitation commonly associated with nanodrug delivery systems.

CONCLUSIONS

In conclusion, a novel dual-phase nanoformulation (NE-RSV+GNP-RSV) was effectively developed for the oral delivery of resveratrol. This formulation significantly improved the bioavailability of simvastatin after 7 days of treatment, evidenced by a 2.7-fold rise in $AUC_{0\text{-}24}$. The improved bioavailability is likely a result of concurrent inhibition of CYP3A enzymes and P-glycoprotein (P-gp). Although GNP-RSV and NE-RSV independently enhance resveratrol's solubility and absorption, their combination allows resveratrol to partition across both oil and aqueous phases,

promoting sustained and more effective inhibition of its metabolic pathways. These results indicated that the NE-RSV + GNP-RSV formulation may serve as a supportive approach to improve the absorption and effectiveness of poorly water-soluble drugs. Further investigation is needed to refine the formulation and evaluate its long-term safety, therapeutic efficacy, and translational applicability in clinical contexts. This strategy may offer a promising solution to address the challenges of oral delivery for drugs and nutraceuticals with inherently low bioavailability.

ACKNOWLEDGEMENTS

The authors acknowledge Dr. M. Gholami's help and support for animal studies.

Free and basic versions of Grammarly and Microsoft Copilot have been applied for occasional correction or rewriting of sentences.

This study was supported by Tehran University of Medical Sciences, Tehran, Iran (Grant No. 1400-3-148-55025). Portions of the manuscript were edited with the assistance of ChatGPT (OpenAI) to improve linguistic clarity and readability.

AUTHOR'S CONTRIBUTION

Akram Hassanpour: Dataset collection, formal analysis, research, technique, software, supplies, validation, original draft writing, review and revision, illustration

Omid Sabzevari: Conceptual Development, Oversight, Methodical Basis, Visual Presentation

Banafsheh Kiani-Dehkordi: Formal analysis, Methodology

Amir Amani: Conceptualization, Methodology, Visualization, Supervision, Writing-Review and Corrections.

Fariba Esmaeili: Methodology, Analysis, and Supplies.

Sharmin Kharrazi: Understanding, Approach, Diagramming, Supervision, Managing Projects, Funding Acquisition, Writing-Review and Editing.

CONFLICT OF INTEREST

The authors report no conflicts of interest.

AVAILABILITY OF RESEARCH DATA

All data generated or examined in this study are entirely included within the published article.

REFERENCES

1. Alqahtani MS, Kazi M, Alsenaidy MA, Ahmad MZ. Advances in oral drug delivery. Front Pharmacol. 2021;12:618411.
2. Petrova E. Innovation in the pharmaceutical industry: The process of drug discovery and development. In: Innovation and Marketing in the Pharmaceutical Industry: Emerging Practices, Research, and Policies. Springer; 2013; 19–81.
3. Wen H, Jung H, Li X. Drug delivery approaches in addressing clinical pharmacology-related issues: opportunities and challenges. AAPS J. 2015;17:1327–1340.
4. Yim D, Kim MJ, Shin Y, Lee SJ, Shin JG, Kim DH. Inhibition of cytochrome P450 activities by Sophora flavescens extract and its prenylated flavonoids in human liver microsomes. Evid Based Complement Alternat Med. 2019;2019.
5. Hyrsova L, Vanduchova A, Dusek J, Smutny T, Carazo A, Maresova V, et al. Trans-resveratrol, but not other natural stilbenes occurring in food, carries the risk of drug-food interaction via inhibition of cytochrome P450 enzymes or interaction with xenosensor receptors. Toxicol Lett. 2019;300:81–91.
6. Chan WK, Delucchi AB. Resveratrol, a red wine constituent, is a mechanism-based inactivator of cytochrome P450 3A4. Life Sci. 2000;67(25):3103–3112.
7. Lee SY, Lee JY, Kang W, Kwon KI, Oh SJ, Ma JY, et al. In vitro and in vivo assessment of cytochrome P450-mediated herb-drug interaction of Ssang-hwa-tang. Food Chem. 2013;136(2):450–457.
8. Tiwari SB, Amiji MM. Improved oral delivery of paclitaxel following administration in nanoemulsion formulations. J Nanosci Nanotechnol. 2006;6(9–10):3215–3221.
9. Basheer L, Schultz K, Kerem Z. Inhibition of cytochrome P450 3A by acetoxylated analogues of resveratrol in in vitro and in silico models. Sci Rep. 2016;6(1):31557.
10. Al-Hamadani MYI, Alzahrani AM, Yousef MI, Kamel MA, El-Sayed WM. Gold nanoparticles perturb drug-metabolizing enzymes and antioxidants in the livers of male rats: potential impact on drug interactions. Int J Nanomedicine. 2020;15:5005–5016.
11. Inbaraj BS, Hua L-H, Chen B-H. Comparative study on inhibition of pancreatic cancer cells by resveratrol gold nanoparticles and a resveratrol nanoemulsion prepared from grape skin. Pharmaceutics. 2021;13(11):1871.
12. Dzimitrowicz A, Bielawska-Pohl A, Pohl P, Jermakowicz-Bartkowiak D, Jamroz P, Malik-Gajewska M, et al. Application of oil-in-water nanoemulsion carrying size-defined gold nanoparticles synthesized by non-thermal plasma for the human breast cancer cell lines migration and apoptosis. Plasma Chem Plasma Process. 2020;40(4):1037–1062.
13. Sereemaspu A, Hongpitich P, Rojanathan R, Maneewatta P, Ekgasit S, Warisnoich W. Inhibition of human cytochrome P450 enzymes by metallic nanoparticles: a preliminary to nanogenomics. Int J Pharmacol. 2008;4(6):492–495.
14. Niżnik Ł, Noga M, Kobylarz D, Frydrych A, Krośniak A, Kapka-Skrzypczak L, et al. Gold nanoparticles (AuNPs)—toxicity, safety and green synthesis: a critical review. Int J Mol Sci. 2024; 25(7): 4057.
15. Balasubramanian D, Girigoswami A, Girigoswami K.

Nano resveratrol and its anticancer activity. Curr Appl Sci Technol. 2022;23(3).
16. Pangeni R, Sharma S, Mustafa G, Ali J, Baboota S. Vitamin E loaded resveratrol nanoemulsion for brain targeting for the treatment of Parkinson's disease by reducing oxidative stress. Nanotechnology. 2014; 25(48): 485102.
17. Fayazbakhsh F, Hataminia F, Eslam HM, Ajoudanian M, Kharrazi S, Sharifi K, et al. Evaluating the antioxidant potential of resveratrol-gold nanoparticles in preventing oxidative stress in endothelium on a chip. Sci Rep. 2023; 13(1): 21344.
18. Sanna V, Siddiqui IA, Sechi M, Mukhtar H. Resveratrol-loaded nanoparticles based on poly(epsilon-caprolactone) and poly(D,L-lactic-co-glycolic acid)-poly(ethylene glycol) blend for prostate cancer treatment. Mol Pharm. 2013; 10(10): 3871–3881.
19. Zhang X, Chen S, Luo D, Chen D, Zhou H, Zhang S, et al. Systematic study of resveratrol nanoliposomes transdermal delivery system for enhancing anti-aging and skin-brightening efficacy. Molecules. 2023; 28(6): 2738.
20. Hirota T, Fujita Y, Ieiri I. An updated review of pharmacokinetic drug interactions and pharmacogenetics of statins. Expert Opin Drug Metab Toxicol. 2020; 16(9): 809–822.
21. Danaei M, Dehghankhold M, Ataei S, Hasanzadeh Davarani F, Javanmard R, Dokhani A, et al. Impact of particle size and polydispersity index on the clinical applications of lipidic nanocarrier systems. Pharmaceutics. 2018; 10(2): 57.
22. Adan A, Kiraz Y, Baran Y. Cell proliferation and cytotoxicity assays. Curr Pharm Biotechnol. 2016; 17(14): 1213–1221.
23. Ma B, Wang J, Sun J, Li M, Xu H, Sun G, et al. Permeability of rhynchophylline across human intestinal cell in vitro. Int J Clin Exp Pathol. 2014; 7(5): 1957–1966.
24. Marino AM, Yarde M, Patel H, Chong S, Balimane PV. Validation of the 96 well Caco-2 cell culture model for high throughput permeability assessment of discovery compounds. Int J Pharm. 2005; 297(1–2): 235–241.
25. Hunter J, Hirst BH, Simmons NL. Drug absorption limited by P-glycoprotein-mediated secretory drug transport in human intestinal epithelial Caco-2 cell layers. Pharm Res. 1993; 10(5): 743–749.
26. Press B, Di Grandi D. Permeability for intestinal absorption: Caco-2 assay and related issues. Curr Drug Metab. 2008; 9(9): 893–900.
27. Jacob Filho W, Lima CC, Paunksnis MRR, Silva AA, Perilhão MS, Caldeira M, et al. Reference database of hematological parameters for growing and aging rats. Aging Male. 2018; 21(2): 145–148.
28. Delwatta SL, Gunatilake M, Baumans V, Seneviratne MD, Dissanayaka MLB, Batagoda SS, et al. Reference values for selected hematological, biochemical and physiological parameters of Sprague-Dawley rats at the Animal House, Faculty of Medicine, University of Colombo, Sri Lanka. Anim Model Exp Med. 2018; 1(4): 250–254.
29. Shete NA, Pawar A, Lokhande V, Swami V. Polyphenols: the interactions with CYP450 isoenzymes and effect on pharmacokinetics of drugs. Pharm Reson. 2022; 4(2).
30. Hyrsova L, Vanduchova A, Dusek J, Smutny T, Carazo A, Maresova V, et al. Trans-resveratrol, but not other natural stilbenes occurring in food, carries the risk of drug-food interaction via inhibition of cytochrome P450 enzymes or interaction with xenosensor receptors. Toxicol Lett. 2019; 300: 81–91.
31. Singh Y, Meher JG, Raval K, Khan FA, Chaurasia M, Jain NK, et al. Nanoemulsion: concepts, development and applications in drug delivery. J Control Release. 2017; 252: 28–49.
32. Rao J, McClements DJ. Formation of flavor oil microemulsions, nanoemulsions and emulsions: influence of composition and preparation method. J Agric Food Chem. 2011; 59(9): 5026–5035.
33. Azeem A, Rizwan M, Ahmad FJ, Iqbal Z, Khar RK, Aqil M, et al. Nanoemulsion components screening and selection: a technical note. AAPS PharmSciTech. 2009; 10(1): 69–76.
34. Hochman JH, Pudvah N, Qiu J, Yamazaki M, Tang C, Lin JH, et al. Interactions of human P-glycoprotein with simvastatin, simvastatin acid, and atorvastatin. Pharm Res. 2004; 21(9): 1686–1691.
35. Sharom FJ. The P-glycoprotein multidrug transporter. Essays Biochem. 2011; 50(1): 161–178.
36. Elmeliegy M, Vourvahis M, Guo C, Wang DD. Effect of P-glycoprotein (P-gp) inducers on exposure of P-gp substrates: review of clinical drug-drug interaction studies. Clin Pharmacokinet. 2020; 59(6): 699–714.
37. Kitagawa S. Inhibitory effects of polyphenols on p-glycoprotein-mediated transport. Biol Pharm Bull. 2006;29(1):1-6.
38. Hong SP, Choi DH, Choi JS. Effects of resveratrol on the pharmacokinetics of diltiazem and its major metabolite, desacetyldiltiazem, in rats. Cardiovasc Ther. 2008; 26(4): 269–275.
39. Bedada SK, Yellu NR, Neerati P. Effect of resveratrol on the pharmacokinetics of fexofenadine in rats: Involvement of P-glycoprotein inhibition. Pharmacol Rep. 2016;68(2):338-343.
40. Marino AM, Yarde M, Patel H, Chong S, Balimane PV. Validation of the 96 well Caco-2 cell culture model for high throughput permeability assessment of discovery compounds. Int J Pharm. 2005; 297(1–2): 235–241.
41. Al-Abd AM, Mahmoud AM, El-Sherbiny GA, El-Moselhy MA, Nofal SM, El-Latif HA, et al. Resveratrol enhances the cytotoxic profile of docetaxel and doxorubicin in solid tumour cell lines in vitro. Cell Prolif. 2011; 44(6): 591–601.
42. Hunter J, Hirst BH, Simmons NL. Drug absorption limited by P-glycoprotein-mediated secretory drug transport in human intestinal epithelial Caco-2 cell layers. Pharm Res. 1993; 10(5): 743–749.
43. Nabekura T, Kamiyama S, Kitagawa S. Effects of dietary chemopreventive phytochemicals on P-glycoprotein function. Biochem Biophys Res Commun. 2005;327(3):866-870.
44. Verma M, Nanda A, Kumar Y. Self-emulsifying drug

delivery system of simvastatin: formulation development, optimization by Box-Behnken design, in-vitro and in-situ single-pass intestinal perfusion (SPIP) studies. Recent Pat Drug Deliv Formul. 2018; 12(3): 199–211.
45. Jacob Filho W, Lima CC, Paunksnis MRR, Silva AA, Perilhão MS, Caldeira M, Bocalini D, de Souza RR. Reference database of hematological parameters for growing and aging rats. Aging Male. 2018;21(2):145-148.
46. Edwards JA, Beck M, Riegger C, Bausch J. Safety of resveratrol with examples for high purity, trans-resveratrol, resVida®. Ann N Y Acad Sci. 2011; 1215: 131–137.
47. Mitschke D, Reichel A, Fricker G, Moenning U. Characterization of cytochrome P450 protein expression along the entire length of the intestine of male and female rats. Drug Metab Dispos. 2008; 36(6): 1039–1045.
48. Zhou SF, Xue CC, Yu XQ, Li C, Wang G. Clinically important drug interactions potentially involving mechanism-based inhibition of cytochrome P450 3A4 and the role of therapeutic drug monitoring. Ther Drug Monit. 2007; 29(6): 687–710.
49. Vaghasiya JD, Bhalodia YS, Manek RA, Gohil TA, Rathod SP. Oxidative stress mediated hepatotoxicity produced by simvastatin. Pharmacologyonline. 2008; 3: 495–503.
50. Yorulmaz H, Ozkok E, Erguven M, Ates G, Aydın I, Tamer S. Effect of simvastatin on mitochondrial enzyme activities, ghrelin, hypoxia-inducible factor 1α in hepatic tissue during early phase of sepsis. Int J Clin Exp Med. 2015;8(3):3640–3650.
51. Motawi TK, Teleb ZA, El-Boghdady NA, Ibrahim SA. Effect of simvastatin and naringenin coadministration on rat liver DNA fragmentation and cytochrome P450 activity: an in vivo and in vitro study. J Physiol Biochem. 2014; 70(1): 225–237.
52. Piver B, Berthou F, Dreano Y, Lucas D. Differential inhibition of human cytochrome P450 enzymes by epsilon-viniferin, the dimer of resveratrol: comparison with resveratrol and polyphenols from alcoholized beverages. Life Sci. 2003; 73(9): 1199–1213.
53. Chi YC, Lin SP, Hou YC. A new herb-drug interaction of Polygonum cuspidatum, a resveratrol-rich nutraceutical, with carbamazepine in rats. Toxicol Appl Pharmacol. 2012; 263(3): 315–322.
54. Yang SY, Tsai SY, Hou YC, Chao PLD. Inductive modulation on P-glycoprotein and cytochrome 3A by resveratrol, a constituent of grapes. Food Chem. 2012; 133(3): 683–688.
55. Ye M, Tang L, Luo M, Zhou J, Guo B, Liu Y, Chen B. Size- and time-dependent alteration in metabolic activities of human hepatic cytochrome P450 isozymes by gold nanoparticles via microsomal coincubations. Nanoscale Res Lett. 2014; 9: 642.
56. Detampel P, Beck M, Krähenbühl S, Huwyler J. Drug interaction potential of resveratrol. Drug Metab Rev. 2012; 44(3): 253–265.